9-2010

Statistical Methods for Automatic Crack Detection Based on Vibrothermography Sequence-of-Images Data

Ming Li
Iowa State University

Stephen D. Holland
Iowa State University, sdh4@iastate.edu

William Q. Meeker
Iowa State University, wqmeeker@iastate.edu

Statistical Methods for Automatic Crack Detection Based on Vibrothermography Sequence-of-Images Data

Abstract
Vibrothermography is a relatively new nondestructive evaluation technique for finding cracks through frictional heat generated from crack surface vibrations under external excitations. The vibrothermography inspection method provides a sequence of infrared images as output. We use a matched filter technique to increase the signal-to-noise ratio of the sequence-of-images data. An automatic crack detection criterion based on the features extracted from the matched filter output greatly increases the sensitivity of the vibrothermography inspection method. In this paper, we develop a three dimensional matched filter for the sequence-of-images data, present the statistical analysis for the matched filter output, and evaluate the probability of detection. Our results show the crack detection criterion based on the matched filter output provides improved detection capability.

Keywords
Image analysis, Matched filter, Nondestructive evaluation, Probability of detection, Signal-to-noise ratio

Comments
This is a pre-print of an article from *Applied Stochastic Models in Business and Industry* 26, no. 5 (September/October 2010): 481–495, doi:10.1002/asmb.866.

Statistical Methods for Automatic Crack Detection Based on Vibrothermography Sequence-of-Images Data

Ming Li[1], Stephen D. Holland[2], and William Q. Meeker[1]

[1]Department of Statistics and Center for Nondestructive Evaluation,

Iowa State University, Ames, IA 50011

[2]Department of Aerospace Engineering and Center for Nondestructive Evaluation,

Iowa State University, Ames, IA 50011

Abstract:

Vibrothermography is a relatively new nondestructive evaluation technique for finding cracks through frictional heat generated from crack surface vibrations under external excitations. The vibrothermography inspection method provides a sequence of infrared images as output. We use a matched filter technique to increase the signal-to-noise ratio of the sequence-of-images data. An automatic crack detection criterion based on the features extracted from the matched filter output greatly increases the sensitivity of the vibrothermography inspection method. In this paper, we develop a three dimensional matched filter for the sequence-of-images data, present the statistical analysis for the matched filter output, and evaluate the probability of detection. Our results show the crack detection criterion based on the matched filter output provides improved detection capability.

Key words: Image analysis, Matched filter, Nondestructive evaluation, Probability of detection, Signal-to-noise ratio.

1 INTRODUCTION

1.1 Background

Nondestructive evaluation (NDE) methods are widely used in many industries, such as aerospace applications, to detect defects or cracks enclosed in structures by non-intrusive physical measurements. There exists random measurement noise for most NDE applications and statistical methods are needed for NDE data analysis. MIL-HDBK-1823A [1] describes the standard statistical methods used in NDE applications. Vibrothermography is an NDE inspection method based on the heat generation and temperature change around the defects or cracks under external sonic or ultrasonic wave excitations. The measurement response of a vibrothermography inspection is a sequence of images taken by an infrared camera. The sequence of images record the temporal trend and spatial pattern of temperature changes for the region inspected. Although scalar reduction of the sequence-of-images data is possible (see for example Holland et al. [2]), direct analysis of a set of features presented in the sequence-of-images data has the potential to importantly increase crack detection power.

In this paper we use data obtained by the vibrothermography method, taken on a collection of 63 titanium Ti-6Al-4V specimens containing fatigue cracks. Those titanium specimens were specially fabricated with cracks of known sizes. The background noise for vibrothermography measurements is usually high and a direct view of the sequence-of-images data after standard background removal procedures has, for small cracks, only limited power of discriminating inspection regions that do or do not have cracks. A matched filter can be used to increase the signal-to-noise ratio (SNR) if one has knowledge of the expected signal profile. For the vibrothermography measurement data used in this paper, we use an empirically-derived spatial-temporal profile of the temperature changes to construct a matched filter and the output from the

matched filter provides important improvements in the SNR when compared with the sequence-of-image input data with background removal.

1.2 Related Literature

Olin and Meeker [3] and Spencer [4] provided an overview of statistical methods for NDE techniques. MIL-HDBK-1823A [1] described the standard statistical procedures for scalar NDE data analyses and Annis [5] provided an R package to implement these procedures through the maximum likelihood (ML) method. Wang and Meeker [6] extended the commonly-used scalar detection criterion to a bivariate detection criterion for NDE data with two response variables. Nieters et al. [7] discussed an SNR-based detection criterion for NDE image data analysis. Maldague [8] presented a general introduction for the vibrothermography method in NDE applications. Holland et al. [2] discussed the reduction of a sequence-of-images vibrothermography data to a scalar detection criterion. Turin [9] gave an introduction to matched filter and Engelbery [10] describes the properties of matched filters for stationary noise.

1.3 Overview

The rest of this paper is organized as follows. Section 2 presents the standard statistical methods used in NDE and the concept of probability of detection (POD). Section 3 describes the experimental setup for the vibrothermography inspection system. Section 4 summaries the matched filter technique. Section 5 describes the construction of a matched filter for the vibrothermography sequence-of-images data. Section 6 presents the matched filter output dimension reduction. Section 7 describes the two detection criteria. Section 8 presents the POD comparison results. Section 9 contains some concluding remarks and extensions for future research work.

2 STANDARD STATISTICAL METHODS IN NDE

In this section, we outline the standard statistical methods and procedures for a continuous scalar response in NDE applications, as described at MIL-HDBK-1823A [1]. We will use these methods in our comparison with the methods developed here.

2.1 Signal Response

We use Y to denote the NDE measurement response and a to denote the crack size. Then the statistical model is $h_Y(Y) = \beta_0 + \beta_1 h_a(a) + \varepsilon$ where $h_Y(Y)$ and $h_a(a)$ are specified transformations of the response and flaw size, respectively, β_0 and β_1 are regression parameters, and ε is the measurement error following a normal distribution $N\left(0, \sigma_\varepsilon^2\right)$. With the measurement data (possibly censored or truncated), estimates of the parameter vector $\left(\hat{\beta}_0, \hat{\beta}_1, \hat{\sigma}_y^2\right)$ and the estimated variance covariance matrix of these estimates can be obtained through standard maximum likelihood (ML) statistical methods. Annis [5] provided an R package based on the ML method for this and more general linear regression models with censored observations. It is common to use a normal distribution to describe the variability in ε, although it is possible to use an alternative appropriate distributions when needed. It is possible to use more sophisticated models that are, in some cases, suggested by the physics of the inspection method. In many such cases, however, a simple linear regression model will provide an adequate approximation.

2.2 Detection Threshold

For specimens without any defects there are still measurement responses due to background noise and other measurement variations. We use Y_n to denote the resulting noise response (or its

transformation). Often the noise, which we denote by Y_n, can be modeled adequately with a normal distribution. That is, $Y_n \sim N\left(\mu_n, \sigma_n^2\right)$. NDE data taken on units without cracks or from those regions of a unit not containing a crack provide noise data from which estimates $\left(\hat{\mu}_n, \hat{\sigma}_n^2\right)$ of the noise parameter can be obtained. The detection threshold $\left(y_{th}\right)$ is typically set to provide an acceptably small probability (p_f) of false alarm (e.g., $p_f = 0.01$ or 0.05). In particular, the detection threshold can be chosen such that $\Pr\left(Y_n > y_{th}\right) = p_f$. Thus the detection threshold is then chosen as $y_{th} = \hat{\mu}_n + \hat{\sigma}_n \Phi^{-1}\left(1 - p_f\right)$ where $\Phi^{-1}\left(x\right)$ is the standard normal quantile function.

2.3 POD

For a specified detection threshold, the probability of detection as function of crack size can be obtained as follows:

$$\mathrm{POD}\left(a\right) = \Pr\left(Y > y_{th}\right) = \Phi\left(\frac{\beta_0 + \beta_1 h_a(a) - h_Y(y_{th})}{\sigma_\varepsilon}\right) \tag{1}$$

where $\Phi\left(z\right)$ is the standard normal cumulative distribution function. With knowledge of the estimated variance-covariance matrix of $\left(\hat{\beta}_0, \hat{\beta}_1, \hat{\sigma}_y^2\right)$, confidence bounds for the POD can be obtained by using the delta method (see for example Meeker and Escobar [11], Appendix B).

3 VIBROTHERMOGRAPHY INSPECTION SYSTEM

The particular vibrothermography inspection system that was used in our experiments is illustrated conceptually in Figure 1 (left). This system involves an excitation source, an infrared camera and a laser vibrometer. The excitation source (a piezo stack) is pneumatically pressed to

the sample, and the sample itself is gripped with a rigid or compliant clamp. A coupling medium, such as plastic, is used to separate the tip of the vibration source from the sample. The energy provided by the excitation source causes vibration which in turn causes the crack surfaces to rub and generate heat. The sequence of infrared images, reflecting the sample-surface temperature, is recorded by the infrared camera and the sample-surface velocity is measured by the laser vibrometer. The piezo stack that is used as the excitation source typically generates 1 to 2 kW of vibrational power at a fixed frequency such as 20 kHz. The excitation amplitude is tunable in our system and we used three excitation amplitudes $(1.5, 2.2, 3.0)$ in the experiments. Higher excitation amplitude generates more vibrational power. During an inspection, the vibrational excitation power is coupled into the specimen and the frictional rubbing between crack surfaces generates heat. Both the temperature and the surface velocity are typically recorded at short time intervals for each measurement. In our experiments, the infrared camera sampling rates was 90 Hz and the vibrometer sampling rate was 1 MHz.

The infrared camera takes 150 frames of image for each measurement with the excitation source turning on at frame 20 and turning off at frame 110. The temperature background was obtained by averaging the first 10 frames of the image. The background removal procedure was performed by subtracting the temperature background from each of the 150 frames. Frame 109 was the last frame acquired before the excitation source is turned off and this frame has the highest image contrast.

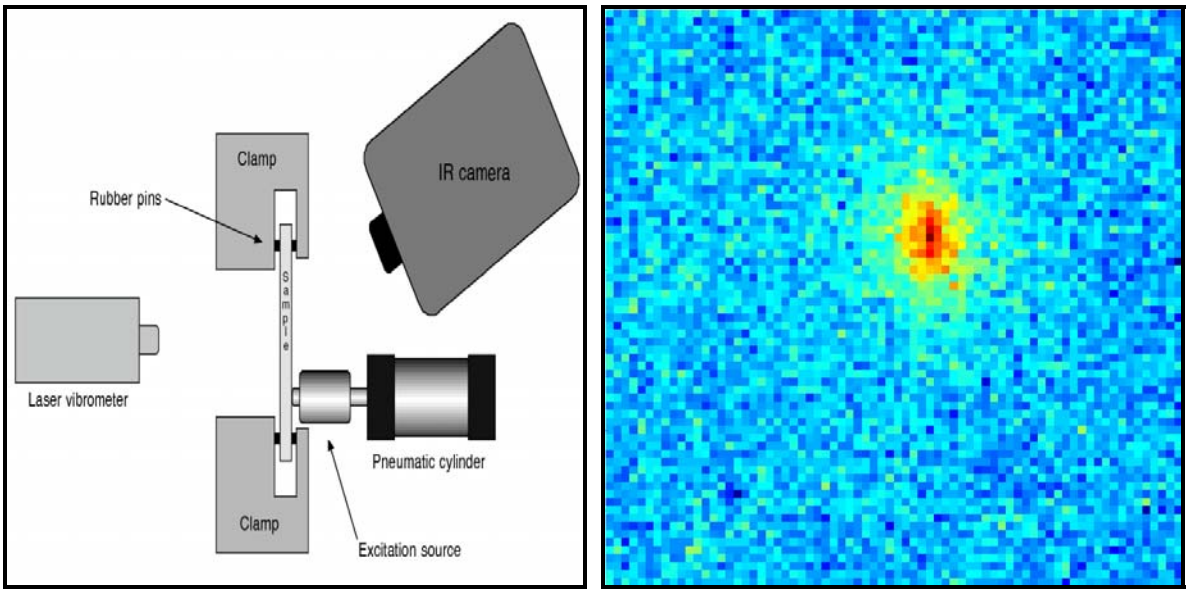

Figure 1. The vibrothermography inspection system setup (left) and a typical spatial pattern image at the frame with highest contrast for a relatively large crack (right).

Figure 1 (right) shows frame 109 (i.e. the frame with the highest image contrast) of the sequence-of-images data after background removal for a relatively large crack. We can clearly see the higher temperature at the center of the picture compared with the surrounding areas, and there would be no problem detecting the existence of a crack from the sequence of images from that particular inspection. In general, however, it is important to identify relatively small cracks where the signal within the sequence of images is usually at or close to the noise level and we cannot easily identify the existence of such cracks. Thus the use of statistical methods to boost SNR is needed to setup crack detection criteria with improved sensitivity needed to develop an automatic crack detection algorithm.

4 CONCEPT OF MATCHED FILTER

The matched filter technique is widely used in signal processing to increase the SNR. An introduction to the matched filter concept can be found in Turin [9]. A matched filter is the

optimal linear filter in terms of improving SNR under a stationary white noise process (see for example Engelbery [10]). One requirement for using a matched filter is the need to construct the filter based on the knowledge of the profile of the signal to be detected. In this section we first show conceptually how a matched filter works in a simple one dimensional (1D) example. Then we extend the method to a more complex 3D situation, corresponding to our application.

4.1 A One Dimensional Matched Filter

Suppose that in 1D, the signal we are expecting to receive is represented by a set of discrete data points $f[k], k = 1,..., N$ as shown by filled circles at Figure 2 (left) with $N = 50$. The 1D white noise is represented by filled triangles and the actual measurement (i.e. signal plus noise) is represented by open squares. We denote the discrete input data (e.g. filled triangles or open squares) by $x[k], k = 1,..., N$. By looking at Figure 2 (left) directly, it is difficult to distinguish between the signal plus noise data (open squares) and the noise-only data (filled triangles), especially when the noise level is high. The matched filter technique utilizes the information of the signal signature to increase the SNR by computing the convolution

$$y[j] = \sum_{k=-\infty}^{\infty} f[j-k] \bullet x[k]$$

as output, where $x[k]$ is the input data (which could be either signal with noise or noise only) and $f[j-k]$ is the reversed known signal (i.e., the matched filter) to be detected. The input data and the matched filter are all discrete-time finite-length arrays. Thus the infinite summation is truncated to be finite and the number of nonzero elements of the output is twice the number of input elements (i.e. $y[j]$, $j = 1,..., 2N$).

The matched filter output results for signal plus noise (open squares) and pure white noise (filled triangles) in Figure 2 (left) are shown in Figure 2 (right) with the same symbolic representation. The matched filter output results for the pure signal are shown in Figure 2 (right) also by filled circles. There is a significant difference between the matched filter output of signal plus noise (open squares) and the pure noise (filled triangles). By applying the matched filter, the SNR for the output of the actual measurement is increased importantly. The best discrimination occurs at the output sequence index $N = 50$, just after all of the information has entered the filter convolution (see for example Engelberg [10]). With the matched filter output results, a reliable automatic classification algorithm can be developed to separate measurement with expected signal and measurement of pure noise.

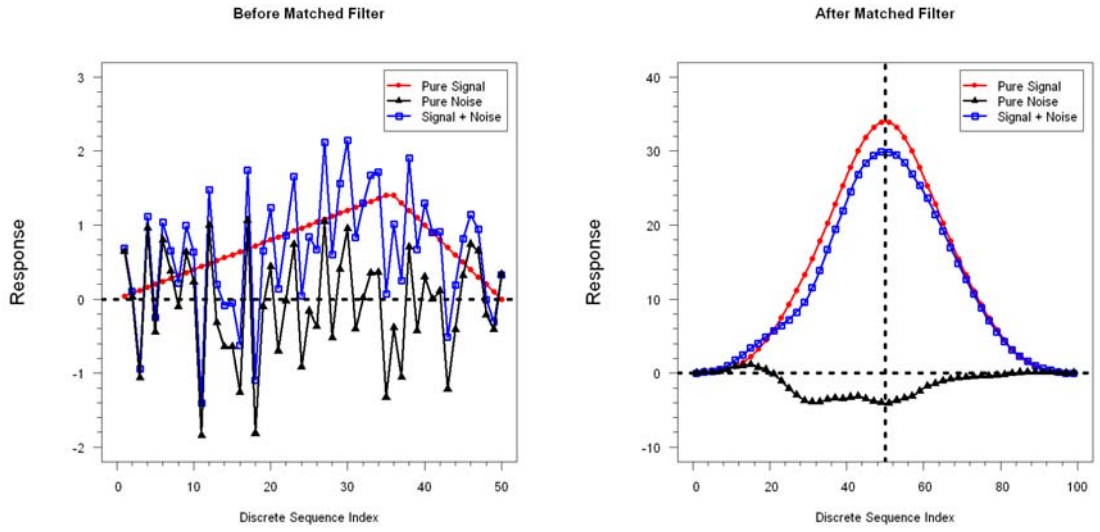

Figure 2. The one dimensional signal, noise and actual measurement input (left) and the output of signal, noise and actual measurement after applying matched filter (right). The discrete symbols in the plot on the right show only the odd number output elements.

4.2 A Three Dimensional Matched Filter

One can extend the 1D matched filter to higher dimensions such as 2D for image analysis and 3D for our sequence-of-images analysis. For our vibrothermography data the known signal profile $f[k_1,k_2,k_3]$ and the input data $x[k_1,k_2,k_3]$ are now three dimensional arrays with $k_1 = 1,...,N_1$, $k_2 = 1,...,N_2$ and $k_3 = 1,...,N_3$. The matched filter is represented by the reversed 3D signal $f[j_1 - k_1, j_2 - k_2, j_3 - k_3]$ and the convolution is now a three-fold summation:

$$y[j_1, j_2, j_3] = \sum_{k_1=-\infty}^{\infty} \sum_{k_2=-\infty}^{\infty} \sum_{k_3=-\infty}^{\infty} f[j_1 - k_1, j_2 - k_2, j_3 - k_3] \bullet x[k_1,k_2,k_3]. \quad (2)$$

For large arrays, the three-fold summation in the convolution is computationally intensive. Fortunately, the Fast Fourier Transformation (FFT) algorithm can be used to reduce the computation time dramatically (see, for example, Brigham [12]). For our sequence-of-images data, the whole computation time to finish one sequence-of-images convolution is less than 10 seconds on a standard PC when using the FFT.

5 MATCHED FILTER FOR VIBROTHERMOGRAPHIC CRACK DETECTION

To construct a 3D matched filter for the sequence-of-images data with background removal, we need to describe the temperature change profile for both the temporal trend and spatial pattern with the presence of a crack. Two approaches can be adopted to get the temperature change profile: (1) use empirical measurements of temperature changes over time and space or (2) use underlying heat-dispersion theory to find the analytical temperature change function.

For the pixels at the center of a medium-size crack, the temperature change trend at each time frame can be obtained with the following procedures. First we take the average of the 2x2 group of pixels at the center of the crack region at each frame to get a sequence of 150 temporal responses. Then we normalize the sequence of temporal responses by dividing the response of frame 109 (i.e. the frame just before the excitation source is turned off). The empirical temporal trend for the center of a typical medium-size crack is shown at Figure 3 (left).

The spatial pattern to represent the temperature changes around the crack is obtained from the normalized 2D Gaussian peak shown at Figure 3 (right). The combination of temporal and spatial characteristics taken together provides the 3D matched filter for the sequence-of-images data.

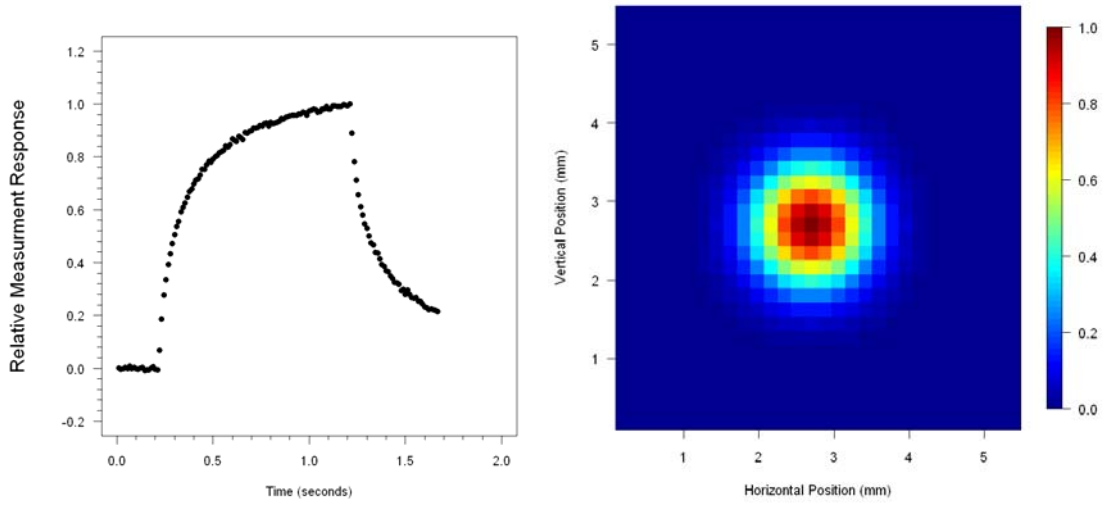

Figure 3. The expected temperature-change profile without noise for matched filter construction: the empirical temporal trend (left) and the Gaussian kernel spatial pattern (right).

6 DIMENSION REDUCTION

6.1 Regions of Signal and Noise

In this paper, we use an SNR-based detection criterion for crack detection. For the specimens used in this laboratory study, we know the location and size of the crack. We will compare the use of the matched filter technique for regions with and without a crack. Also, because we have no specimens without cracks, we will use responses from regions of the specimens without a crack to obtain the noise data. The raw 2D image of frame 109 from the vibrothermography measurement is shown in Figure 4 with the dashed box indicating the location of the entire specimen. The crack is located in the region of the left solid box and the pixels inside the left solid box provide an example of matched filter input data when there is a signal. The pixels inside the right solid box provide an example of matched filter input when there is no signal (i.e., noise data). The same matched filter and detection procedures are used for both regions to assess the performance of our crack detection criterion.

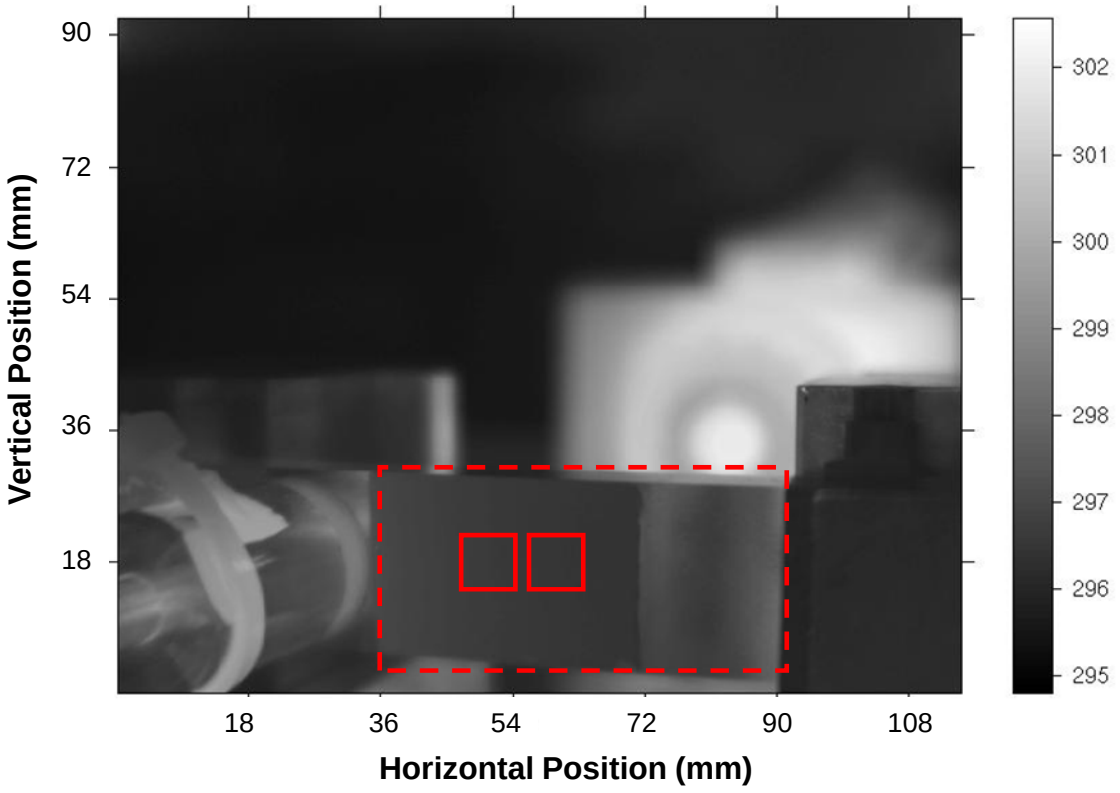

Figure 4. The raw data of the 2D image at frame 109 with the specimen location indicated in the dashed box region. The known crack is located in the region of the left solid box. The pixels in the left solid box are used for the signal matched filter input and the pixels in the right solid box are used for the noise matched filter input.

6.2 Feature Extraction

After applying the matched filter to a background-removed sequence-of-images input, the output is a 3D array with 300 frames of 2D images with the highest contrast image at or near frame 150 (i.e., the frame corresponding to the time at which all the information has entered the filter, similar to sequence index 50 in the 1D example shown in Figure 2 right). Figure 5 (top left) shows the input image of frame 109 (i.e., the last frame with the excitation source turned on) for

an inspection region with a small crack (i.e., the left solid box in Figure 4), and Figure 5 (top right) shows the matched filter output image of frame 150 with a clear “hot spot” indicating the location of the crack. To compare the highest contrast images for noise data, the image of frame 109 of the input data and the image of frame 150 of the output data for an inspection region without a crack (i.e., the right solid box in Figure 4) for the same measurement are shown at Figure 5 (bottom).

Based on a comparison of matched filter outputs for inspection regions with and without a crack for all of the specimens used in the experiment, we developed a noise-threshold detection criterion based on two types of features: (1) the maximum value (MV) in the image of frame 150 after the matched filter as indicated by a cross in Figure 5 (top and bottom right) and (2) an empirical characterization of the noise in a rectangle in the general vicinity of the of the MV (regions between the inner and outer boxes in Figure 5 top and bottom right), represented by the noise peak value and the average noise value of averaging all the pixels in the vicinity region between the two boxes.

In vibrothermography inspection applications, the features obtained from an inspection region (i.e. the MV, and the peak and average noise values) can be used to make crack existence decisions by comparing the MV signal to a threshold that depends on the local noise level. The inspection region is often a rectangle (e.g., the solid boxes illustrated in Figure 4) that is smaller than the specimen. The inspection region is moved around the specimen to cover the entire surface. Adjacent inspection regions are overlapped to avoid edge effects. The detail of the noise threshold detection criterion based on the MV signal, the noise peak value, and average noise value is described at Section 7.2.

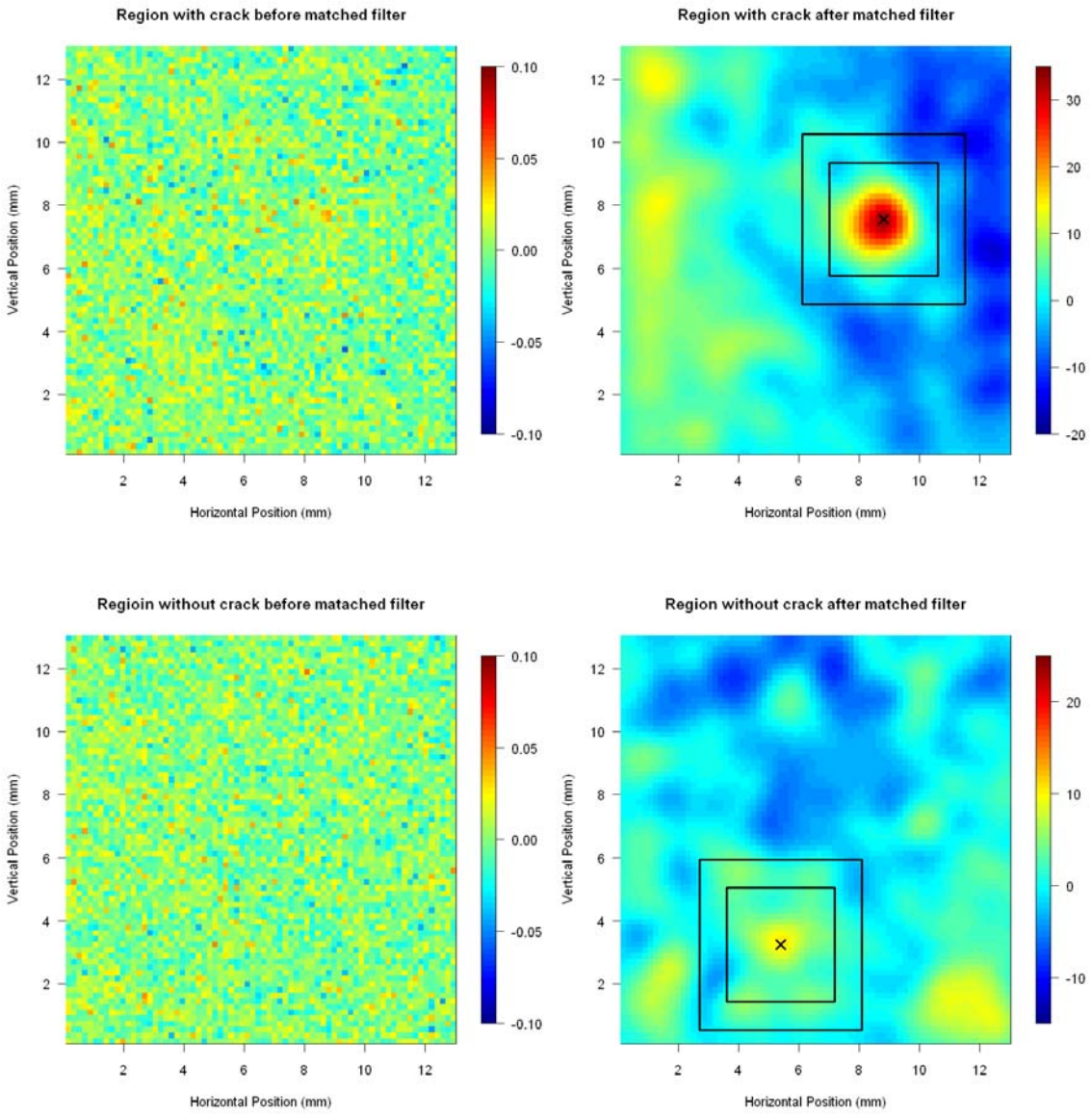

Figure 5. Highest contrast 2D images before (left) and after (right) use of the matched filter for an inspection region with a crack (top) and without a crack (bottom).

7 DETECTION CRITERIA

7.1 Temperature Increase

Holland et al. [2] developed an algorithm to reduce the vibrothermography sequence-of-images data in each measurement into a scalar measure of temperature increase and Li, Holland and Meeker [13]

compared the PODs using the scalar temperature increase for different vibrothermography inspection systems. The algorithm was based on a physical model to perform a surface-fit of the heat from the crack to an elliptical Gaussian envelope. Here we review the method they used to compute POD so that we can compare it with the POD from the matched filter method presented here.

The scalar temperature increase as function of crack size and excitation amplitude is shown at Figure 6 (left). For small cracks, the amount of heat generated is close to the noise level of the inspection system. The same algorithm was applied to regions without a crack to find the noise distribution of the temperature increase. These noise data are independent of the excitation amplitude and are indicated by crosses in Figure 6 (left). The lognormal probability plot for the noise data is shown at Figure 6 (right) indicates the log-transformed temperature increase noise data can be described well by a normal distribution. The detection threshold for temperature increase was determined such that the probability of a false alarm was 0.02 (i.e., no more than 2% of the temperature increase from regions without a crack exceeded the detection threshold). The detection threshold is shown as a horizontal dot-dashed line in Figure 6 (left). The linear regression between temperature increase T, crack size a and excitation amplitude $b = 1.5, 2.2, 3.0$ in the log-log scale is:

$$\log_{10}(T) = \beta_0 + \beta_1 \log_{10}(a) + \beta_2 \log_{10}(b) + \varepsilon_T \tag{3}$$

where β_0, β_1 , β_2 are regression parameters to be estimated from the data and the random variation ε_T is assumed to have a normal distribution $N\left(0, \sigma_T^2\right)$.

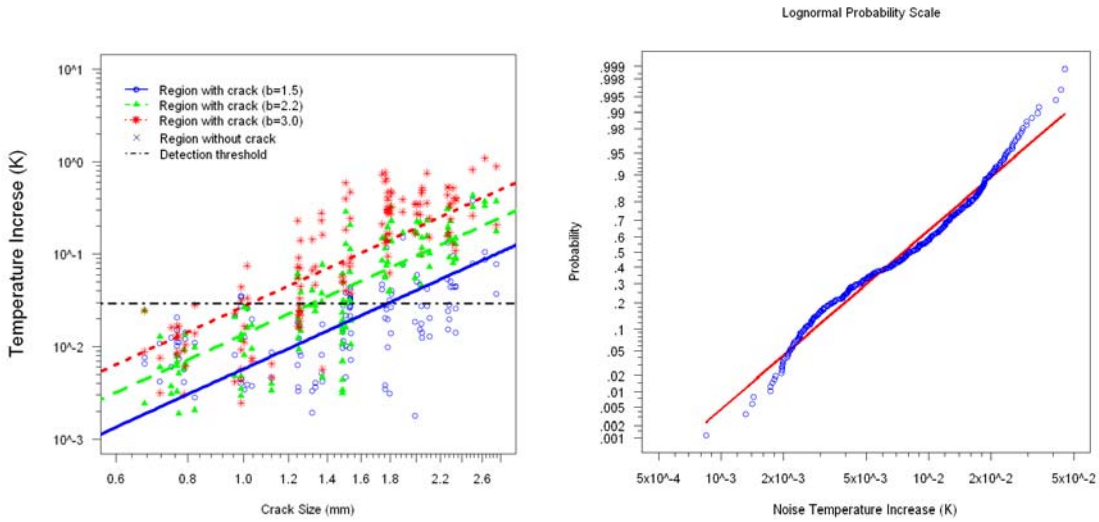

Figure 6. The plot on the left shows scalar temperature increase as function of crack size and excitation amplitude (different symbols). The detection threshold is shown as the horizontal dot-dashed line on the left. The crosses shown on the left are the corresponding noise temperature increase taken in regions of the images where there is no crack. These noise data are also shown in the lognormal probability plot on the right.

7.2 A Detection Criterion Based on Signal and Noise

The concept of a variable-noise threshold was used by Nieters et al. [7] to increase the detection power for C-scan images from ultrasonic inspections of titanium billets. The basic idea is to compare the signal amplitude to a noise threshold that is a function of the estimated noise level in the vicinity of the detection location. By using such a criterion, weak signals caused by small flaws in low-noise areas can still be detected. Here we adapt their idea of a noise-threshold detection criterion to make crack-detection decisions based on the output of the matched filter. Following Nieters et al. [7], the SNR is defined as $\mathrm{SNR} = \left(S_p - N_a\right) / \left(N_p - N_a\right)$ where S_p is the signal maximum value, N_a is the average noise in the surrounding area, and N_p is the peak noise in the surrounding area. The SNR detection criterion is $\mathrm{SNR} > \alpha$ where α may differ depending on the application.

7.2.1 The matched filter signal response

The signal S_p from our matched filter output corresponds to the MV in the image of frame 150 (e.g., the crosses in the middle of the squares in the right-hand plots in Figure 5). The signal S_p from regions with a crack has a strong dependency on crack size and excitation amplitude.

7.2.2 The noise response

We estimate the distribution of noise in the output of our matched filter by using the vicinity region surrounding the MV (i.e. the region between the two boxes in Figure 5 top and bottom right). The maximum value from such region is used to determine the noise peak N_p. The average-noise value from such region is defined as $N_a = \sum \eta_i / M$ where η_i is the response of each pixel in the region and M is the total number of pixels in the region. Following Nieters et al. [7], we define the noise threshold as $N_{th} = \alpha \times N_p + (1-\alpha) \times N_a$ where $\alpha = 2.5$ has been used as the SNR detection criterion in the Multizone ultrasonic inspection of billets and forgings (e.g., Margetan et al. [14]). From the model for our matched filter results, the choice of $\alpha = 3.0$ returns 0.02 probability of a false alarm and $\alpha = 3.0$ is thus used in the SNR detection criterion to compare the performance of noise threshold detection criterion with the scalar temperature increase detection criterion.

7.2.3 The detection criterion

The SNR based detection criterion that declares a find when $\mathrm{SNR} > \alpha$ is equivalent to $\mathrm{S}_p > N_{th}$ or $\log_{10}(\mathrm{S}_p) > \log_{10}(N_{th})$. We define $D = \log_{10}(\mathrm{S}_p) - \log_{10}(N_{th})$ and the observed values of D are shown in Figure 7 (left). The relationship between D and crack size a and the excitation amplitude b is

$$D = \gamma_0 + \gamma_1 \log_{10}(a) + \gamma_2 \log_{10}(b) + \varepsilon_D$$

with regression parameters γ_0, γ_1, γ_2 and the random variation ε_D following a normal distribution $N\left(0, \sigma_D^2\right)$. The detection criterion becomes $D > 0$ and it follows from our model that

$$D \sim N\left(\gamma_0 + \gamma_1 \log_{10}(a) + \gamma_2 \log_{10}(b), \sigma_D^2\right). \tag{4}$$

The normal probability plot for the observed values of $D - \hat{\gamma}_0 - \hat{\gamma}_1 \log_{10}(a) - \hat{\gamma}_2 \log_{10}(b)$ is shown in Figure 7 (right) indicating that the normal distribution assumption in (4) provides a good description of the data.

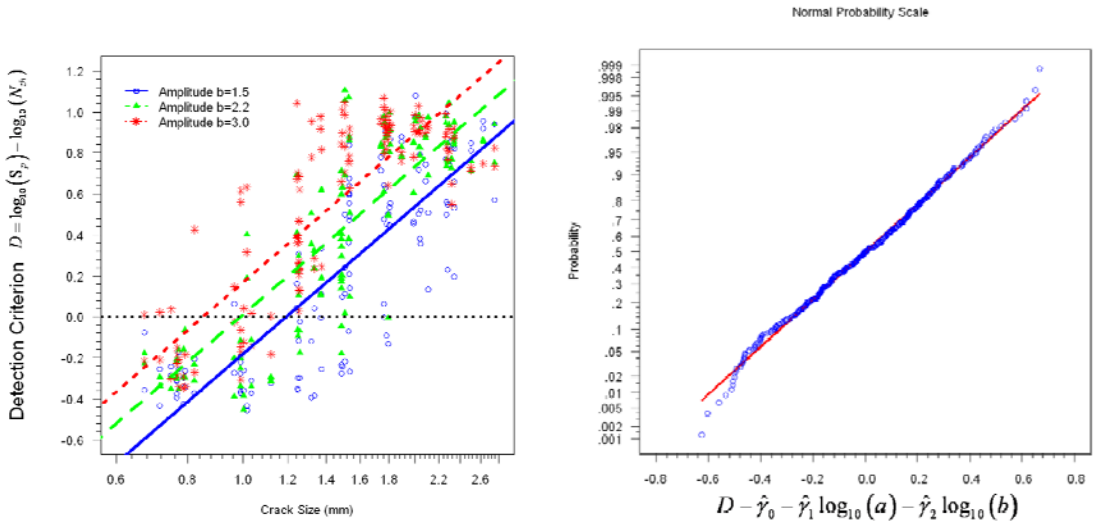

Figure 7. The MV as function of crack size and excitation amplitude (left), and the normal probability plot for the observed values of $D - \hat{\gamma}_0 - \hat{\gamma}_1 \log_{10}(a) - \hat{\gamma}_2 \log_{10}(b)$ (right).

The relationship between the observed MV signal and the noise threshold is shown in Figure 8 for each excitation amplitude with a crack detection criterion being a point above the diagonal dashed line. The dots correspond to inspection regions with a crack and the crosses correspond to inspection regions without a crack. The crosses above the diagonal line are false alarms.

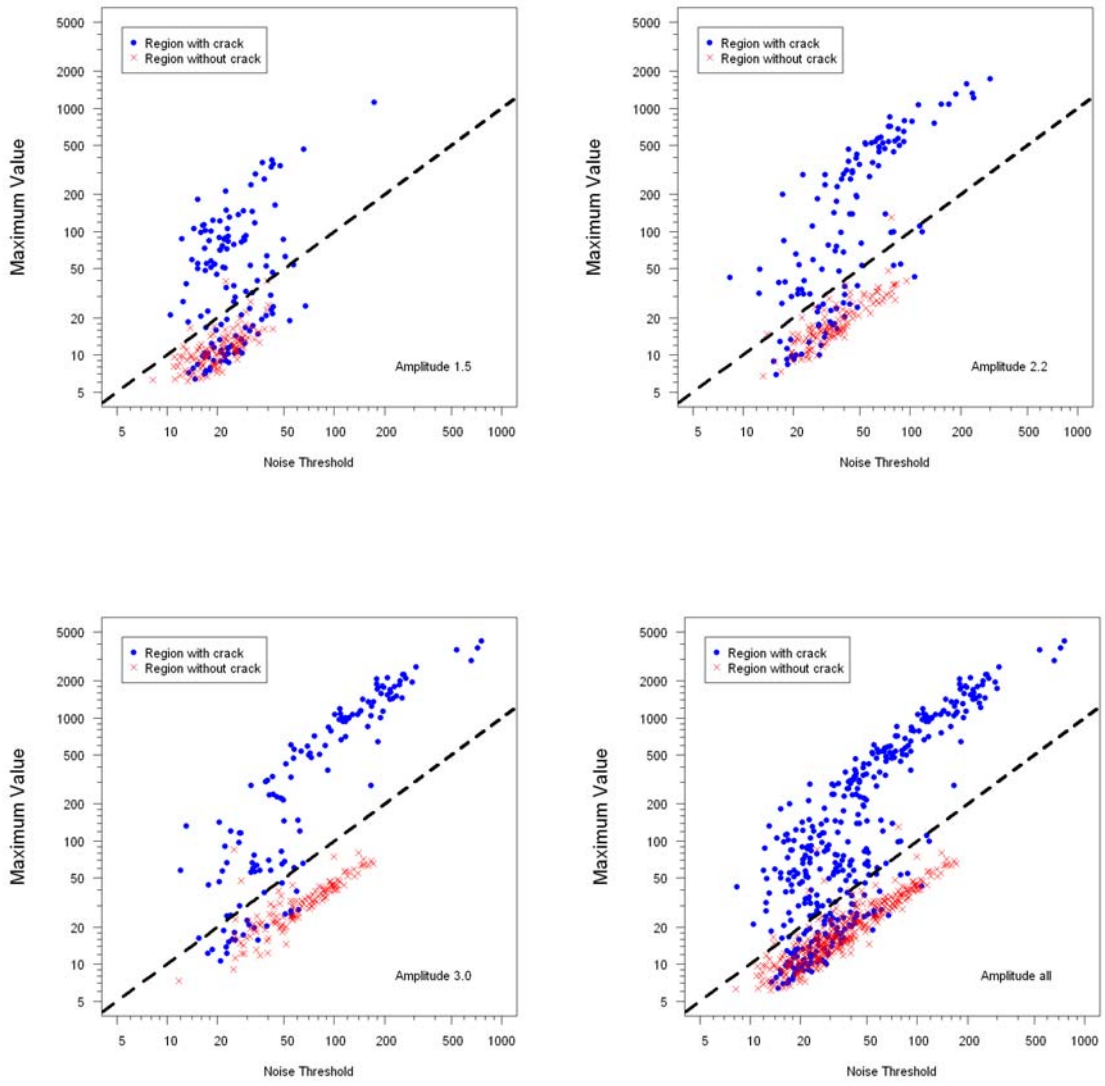

Figure 8. The SNR detection criterion for each excitation amplitude. A detection corresponds to having a MV signal S_p larger than the noise threshold N_{th} (i.e. a point above the diagonal dashed line). The dots correspond to inspection regions with a crack and the crosses correspond to inspection region without a crack.

8 POD COMPARSION

With the log-log linear relationship between the scalar temperature increase, crack size and excitation amplitude in (3) and the detection threshold set such that the probability of a false alarm is 0.02, the POD for the scalar temperature increase detection criterion can be found by using the approach described in Section 2. That is,

$$\mathrm{POD}(a) = \Phi\left(\frac{\beta_0 + \beta_1 \log_{10}(a) + \beta_2 \log_{10}(b) - \log_{10}(y_{T,th})}{\sigma_T}\right)$$

where a is the crack size, $y_{T,th}$ is the detection threshold for temperature increase, and Φ is the standard normal cumulative distribution function. For the detection procedures described in Section 7.2.3, the POD for the SNR-based noise threshold detection criterion is obtained as

$$\mathrm{POD}(a) = \Pr(D > 0) = \Phi\left(\frac{\gamma_0 + \gamma_1 \log_{10}(a) + \gamma_2 \log_{10}(b)}{\sigma_D}\right).$$

The estimated POD and its 95% lower confidence bound (LB) based on both the scalar temperature increase and the matched-filter SNR-based detection criteria are shown at Figure 9 (top left, top right and bottom left) with a solid line for the POD estimate and a dashed line for the POD LB for each excitation amplitude. A POD comparison for all three excitation amplitudes is shown at Figure 9 (bottom right).The comparison shows that the matched-filter SNR-based noise threshold detection criterion provides an overall better POD. Based on the matched-filter SNR-based detection criterion POD, an automatic detection algorithm with $\mathrm{SNR} > 3.0$ will have, with 95% confidence, a probability of at least 0.90 to detect a crack with size 1.21 mm (known as the a90/95 value in the NDE community) for high excitation amplitude. The a90/95 value for the temperature increase detection criterion is 1.65 mm for the high excitation amplitude. Both a90/95 values are indicated by vertical dotted lines in Figure 9.

Compared with the temperature increase criterion, for the same detection confidence (e.g. 95% confidence, a probability of at least 0.90 to detect), the noise threshold criterion can detection cracks 0.44 mm smaller if using high excitation amplitude, and 1.22 mm smaller if using low excitation amplitude.

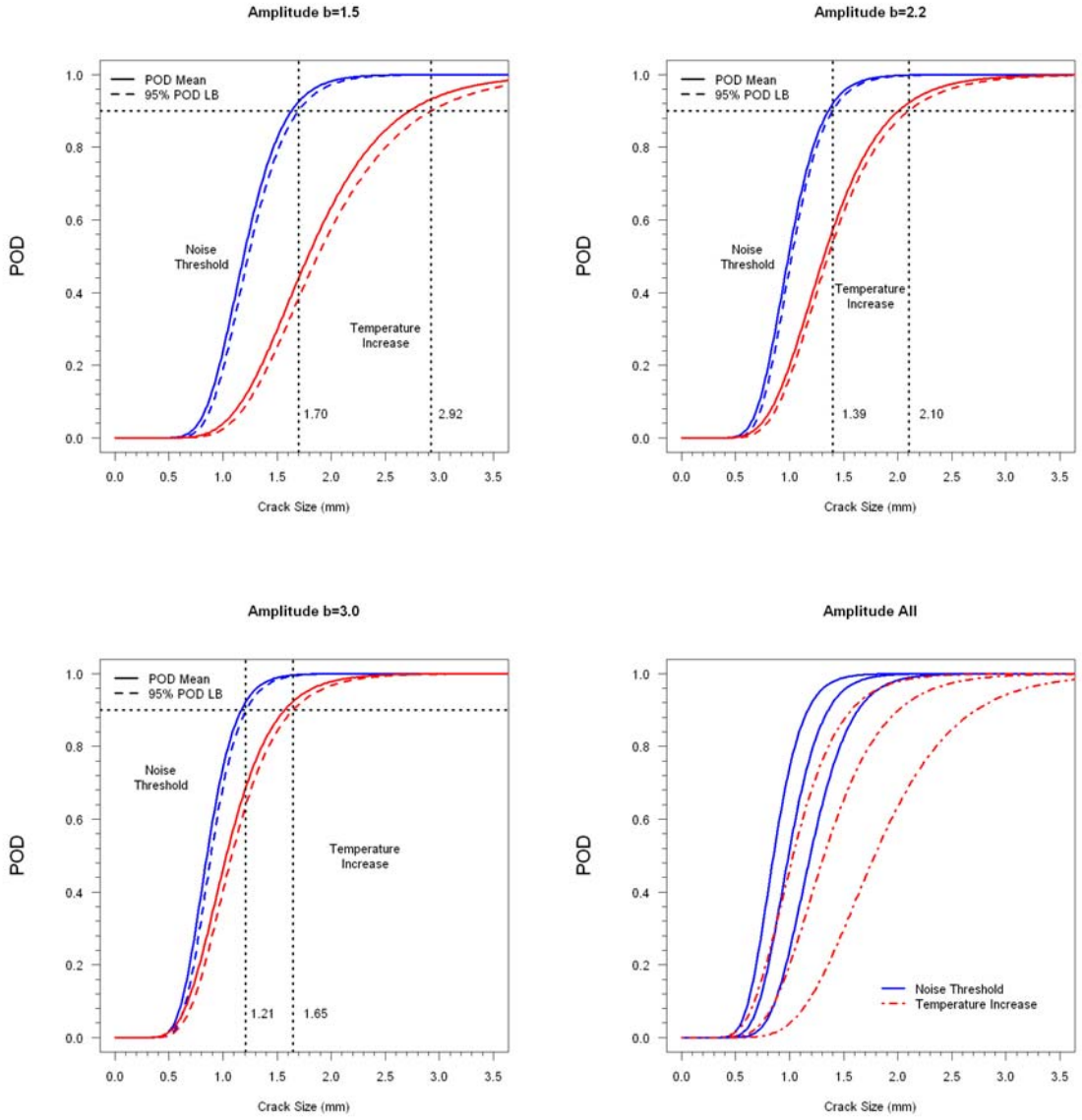

Figure 9. The POD and its 95% LB for temperature increase detection and the matched-filter noise threshold detection with a90/95 value for each excitation amplitude (top left, top right and bottom left), and POD mean comparison for all three excitation amplitudes (bottom right).

9 SUMMARY AND CONCLUSION

In this paper we have developed a 3D matched filter to greatly increase the SNR of the vibrothermography sequence-of-images inspection data. We suggested a matched-filter SNR-based detection. With detection thresholds set to have the same probability of a false alarm, the SNR detection criterion based on the output of the matched filter has better overall detection performance when compared with the scalar temperature increase results from our previous study.

There are a number of possible extensions for the methodology presented in this paper that suggest future research directions. These include the following:

- Our procedure has been applied to vibrothermography sequence-of-images data from just one system configuration. The performance of our procedures with other vibrothermography detection systems on different kinds of specimens needs to be evaluated.
- We now use a normalized Gaussian peak to represent the temporal-spatial profile. Other types of spatial profiles can be developed to detect particular types of defects such as elongated or triangle shaped cracks.
- It might be possible to find an alternative SNR-based detection criterion that uses the matched filter output in a different manner and that would improve POD without increasing the probability of a false alarm.

ACKNOWLEDGEMENTS

This material used in the paper is based upon work supported by the Air Force Research Laboratory under Contract # FA8650-04-C-5228 at Iowa State University's Center for NDE.

REFERENCES

1. MIL-HDBK-1823A, *Nondestructive Evaluation System Reliability Assessment*, Standardization Order Desk, Building 4D, 700 Roberts Avenue, Philadelphia, PA, 2009.
2. Holland, S. D., Uhl, C., Ouyang, Z., Patton, T., Li, M., Meeker, W. Q., Lively, J., Brasche, L., Eisenmann, D., "Relating vibrothermographic crack heating to crack size and crack motion," to be submitted, 2010.
3. Olin, D. B., Meeker, W. Q., "Application of statistical methods to nondestructive evaluation," *Technometrics* 1996; **38**: 95-112.
4. Spencer, F. W., "Discussion: application of statistical methods to nondestructive evaluation," *Technometrics* 1996; **38**: 122-124.
5. Annis, C., R package: mh1823, Version 2.5.4.2, http://www.statisticalengineering.com/ [01 June 2010]
6. Wang, Y., Meeker, W. Q., "A bivariate regression model for assessment of multizone ultrasonic POD," *Review of Progress in Quantitative Nondestructive Evaluation* 2006; **25**: 1870-1877.
7. Nieters, E. J., Gilmore, R. S., Trzaskos, R. C., Young, J. D., Copley, D. C., Howard, P. J., Keller, M. E., Leach, W. J., "A multizone technique for billet inspection," *Review of Progress in Quantitative Nondestructive Evaluation* 1995; **14:** 2137-2144.
8. Maldague, X. P. V., *Theory and Practice of Infrared Technology for Nondestructive Testing*, Wiley, NY, 2001.
9. Turin, G. L., "An introduction to matched filters," *IRE Transaction on Information Theory* 1960, **6**: 311-329.
10. Engelberg, S., *Random Signals and Noise*, Taylor and Francis, NY, 2007.
11. Meeker, W. Q., Escobar, L. A., *Statistical Methods for Reliability Data*, Wiley, NY, 1998.
12. Brigham, E., *Fast Fourier Transform and Its Applications*, Prentice Hall, NY, 1988.

13. Li, M., Holland, S. D., Meeker, W. Q., “Quantitative multi-inspection-site comparison of probability of detection for vibrothermography nondestructive evaluation data,” submitted 2010.
14. Margetan, F.J., Umbach, J., Roberts, R., Friedl, J., Degtyar, A., Keller, M., Hassan, W., Brasche, L., Klassen, A., Wasan, H., Kinney, A., “Inspection developments for titanium forgings,” DOT/FAA/AR-05/46, Air Traffic Organization Operations Planning Office of Aviation Research and Development, Washington, DC, 2007.